JOURNAL OF MAGNETIC RESONANCE, Series B **111,** 204–207 (1996)
ARTICLE NO. 0084

Hyperpolarized ^{129}Xe MR Imaging of the Oral Cavity

M. S. ALBERT,* C. H. TSENG,*,† D. WILLIAMSON,* E. R. OTEIZA,† R. L. WALSWORTH,† B. KRAFT,* D. KACHER,* B. L. HOLMAN,* AND F. A. JOLESZ*

*Department of Radiology, Brigham and Women's Hospital, Harvard Medical School, Boston, Massachusetts 02115; and †Harvard-Smithsonian Center for Astrophysics Cambridge, Massachusetts 02138

Received March 4, 1996

The demonstration of MR images using hyperpolarized ^{129}Xe has introduced a potential new contrast modality for imaging (*1, 2*). Recently, others obtained hyperpolarized ^{3}He images of the guinea pig lung (*3, 4*) and the human lung (*5*). There is considerable interest in extending the technique to physiological human imaging. As a step toward this, we present the first hyperpolarized xenon images obtained from a human subject: an image of the human oral cavity.

Although ^{129}Xe has a spin-$\frac{1}{2}$ nucleus and is NMR detectable, its relatively low tissue concentration (10^3 times less than water protons), coupled with its low sensitivity, renders conventional imaging approaches useless. The novel technique of noble-gas hyperpolarization, by collisional spin exchange with optically pumped rubidium vapor, yields up to a hundred thousandfold enhancement in detectability (*6–9*). Hyperpolarized xenon MRI (HypX-MRI) offers a new range of exploitable responses and contrast, and promises temporal and spatial resolutions comparable to conventional MRI employing $^{1}H_2O$.

For imagining organs with air spaces, such as the lungs and sinuses, ^{3}He, with its greater gyromagnetic moment, yields an MR signal that is 7.6 times larger than that of ^{129}Xe for a given polarization and equal number of spins, but the extremely low solubility of helium in the blood (*10*) precludes its use for imaging of tissue. Xenon has a solubility in blood an order of magnitude greater than that of helium (*10*). It is lipophilic, as its anesthetic properties would suggest, and achieves high concentrations in lipid-rich tissues (*10*).

For the first tests of HypX-MRI in a human subject, we imaged the oral cavity of a subject inhaling hyperpolarized xenon. The oral cavity can be imaged with the relatively small quantities of hyperpolarized xenon that we are currently able to produce and serves the purposes of a first demonstration. When larger amounts of hyperpolarized xenon become available, imaging the lung gas-space, lung tissue, and various distal organs should be possible.

Natural-abundance xenon gas (26% ^{129}Xe) of research grade purity (99.995%) was acquired from Isotec, Inc. A cylindrical 25 cm^3 Pyrex polarization cell of 2 cm diameter and 7 cm length was coated with octadecyltrichlorosilane (OTS) (*11*) to inhibit the loss of ^{129}Xe hyperpolarization due to collisions of Xe atoms with the container walls. The cell was fitted with high-vacuum O-ring valves and filled with 3 atm of natural xenon, 0.2 atm of nitrogen, and a small ($\sim$mg) quantity of solid rubidium. The polarization cell was maintained at 85°C using a resistively heated oven to achieve an optimum rubidium vapor density of $10^{12}/\text{cm}^3$. The polarization cell was placed in the fringing field of our MRI magnet and illuminated for approximately 30 minutes with high-power ($\sim$20 W), circularly polarized light tuned to the rubidium D1 transition (between the $5^2S_{1/2}$ and $5^2P_{1/2}$ electronic states) at 795 nm from a multistripe GaA1As diode laser array (FWHM $\approx$ 1.5 nm) manufactured by Optopower, Inc. The nitrogen buffer gas collisionally deexcited rubidium atoms in the excited $5^2P_{1/2}$ state, preventing radiation trapping.

Hyperpolarization of ^{129}Xe is achieved through spin-exchange collisions with optically pumped Rb vapor. Absorption of the circularly polarized laser light produces a high electron spin polarization in the rubidium atoms through depopulation optical pumping. Subsequent gas collisions between the rubidium and ^{129}Xe transfer some of this polarization to the ^{129}Xe nuclei. After 30 min of optical pumping and spin exchange, the ^{129}Xe nuclear polarization was roughly 8%, resulting in an MR signal enhancement of about 20,000 times that of thermal equilibrium. The polarization cell was then removed from the oven and transported to the opening of the MRI magnet. The cell was rapidly cooled in ice water and the hyperpolarized ^{129}Xe was condensed from the polarization cell into an evacuated 25 cm^3 cylindrical Pyrex condensation cell that was fitted with a high-vacuum O-ring valve and submerged in liquid nitrogen. T_1 is nearly three hours for frozen ^{129}Xe at $\sim$80 K in a magnetic field above 500 G (*12*). The condensation cell was warmed to room temperature to return the ^{129}Xe to a gaseous state. The condensation/sublimation procedure resulted in about 10% loss of the ^{129}Xe hyperpolarization. The subjects then pressed the opening of the xenon-filled cell to their lips while lying

1064-1866/96 $18.00

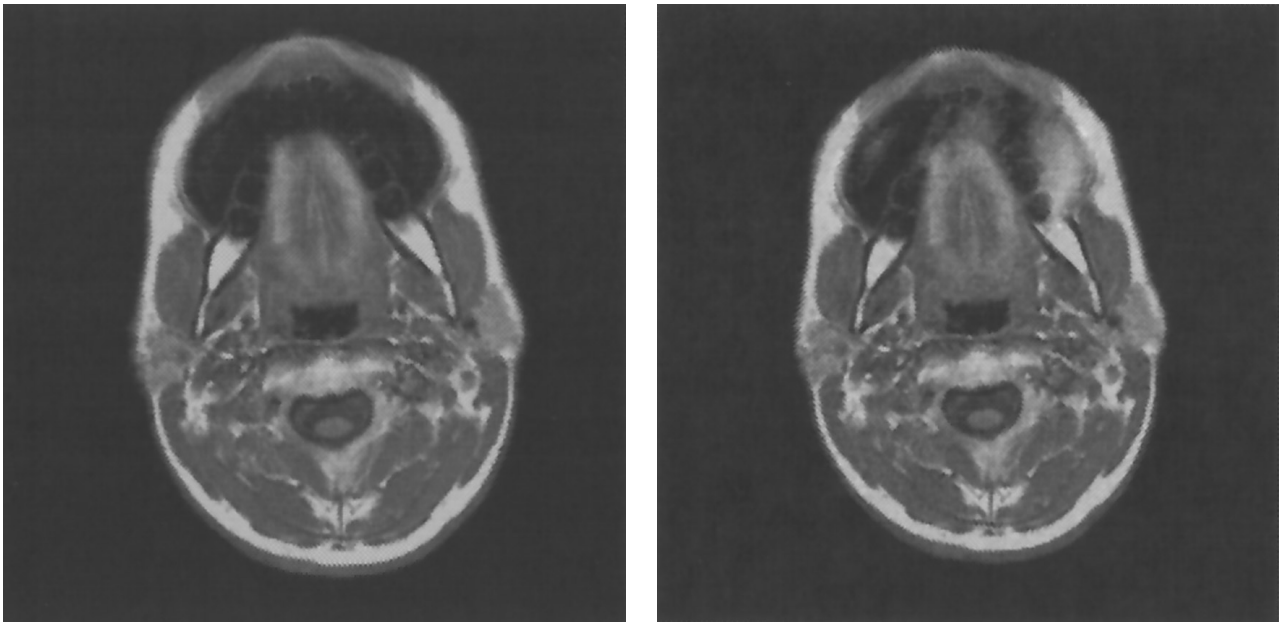

FIG. 1. (Right) Hyperpolarized ^{129}Xe image of an axial slice through the human oral cavity, registered and overlayed onto a corresponding $^{1}H_2O$ image slice. (Left) shows the $^{1}H_2O$ image before overlay. The xenon image was registered to the proton image using the dental ridge and inner cheek lining as references. (Right) shows a bolus of hyperpolarized ^{129}Xe inflating the oral and right buccal cavities (bright relative to the left buccal cavity) of the subject. Note that a signal is void in these cavities in the $^{1}H_2O$ image (left). The ^{129}Xe image closely follows the contour of the teeth and inner cheek. Pixel bit intensities of the xenon image were scaled relative to that of the proton image.

in the MRI scanner and delivered a 50 cm^3 (1 atm) bolus of xenon gas into their mouth by opening the O-ring valve. The xenon was held in the oral cavity of the subjects for the duration of the scan.

Healthy male volunteers were used as subjects. Experimental protocols were previously approved by the Brigham and Women's Hospital Investigative Review Board.

^{129}Xe images were obtained at 17.7 MHz using a 60 cm 1.5 T magnet manufactured by an IBM/MIT/BWH consortium, interfaced with an SMIS computer console. A 4 cm diameter transceiver surface coil was used and the 90° pulse was 100 μs using a 1 kW amplifier. A 2-D gradient-echo sequence was used with a 10° flip angle and a TR of 300 ms. One-centimeter axial slices were obtained through the oral cavity by placing the surface coil against the right cheek. The pixel resolution was 256 $\times$ 128 in an FOV of 40 cm. A spectral width of 10 kHz was used to sample 1K data points. Images were transformed as magnitude values. Axial $^{1}H_2O$ images of the same slice and resolution were obtained on a 1.5 T Signa scanner (GEMS, Milwaukee, Wisconsin) using a birdcage headcoil. A spin-echo sequence with TE of 10 ms, TR of 300 ms, FOV of 24 $\times$ 24 cm, and a pixel matrix of 256 $\times$ 128 was used.

Figure 1 displays an axial hyperpolarized ^{129}Xe image of a slice through the human oral cavity, registered and overlayed onto a conventional water proton MRI of the same slice. The xenon images were registered to the proton images using the dental ridge and inner cheek lining as references. Pixel bit intensities of the xenon image were scaled relative to that of the proton image.

The ^{129}Xe polarization decay time, T_1, in the oral cavity was measured using repetitive single RF excitations with a nominal flip angle of about 1° and a TR of 5 s. T_1 was measured to be about 60 seconds for ^{129}Xe in the oral cavity of the mouth. The relaxation data were fitted by a nonlinear regression method to the function $y = M_0[\exp(-t/T_1)]$. The induced depolarization rate caused by the RF excitations, $|\ln(\cos\theta)|/\mathrm{TR}$, was subtracted from the relaxation rate, $1/T_1$.

The image in Fig. 1 clearly shows a bolus of hyperpolarized ^{129}Xe inflating the oral and right buccal cavities of the subject. Less-intense ^{129}Xe signal can also be seen in the oral cavity directly in front of the tongue and in the left buccal cavity. (The signal strength falls off with distance from the surface coil). The ^{129}Xe image closely follows the contour of the teeth and inner cheek. This composite image demonstrates how HypX-MRI can complement conventional MRI. The imaging of lung gas-space, lung tissue, and distal organs awaits the availability of larger quantities of hyperpolarized xenon.

We are currently testing higher-power lasers and developing an apparatus to produce larger quantities of hyperpolarized ^{129}Xe. One step in this direction is the use of O-ring valve cells. Valved cells are refillable and more convenient than the single-use break-seal cells employed previously (*1, 3*). Because the T_1 of frozen ^{129}Xe is nearly three hours

in the large fields of MR magnets, several polarization cycles can be combined and transferred to a holding cell in order to produce larger amount of hyperpolarized gas.

Imaging with a hyperpolarized noble gas is different in important ways from conventional imaging. The large nonequilibrium polarization of the nuclei is not renewable and requires special considerations when designing suitable imaging pulse sequences. Every excitation pulse destroys some longitudinal magnetization, which then cannot be restored as in conventional MRI by waiting for relaxation back to thermal equilibrium. The disadvantages of such a one-shot procedure are offset by the advantages conferred by the elimination of long recycle delays: high-speed techniques can be utilized that are especially suited to the tracking of physiological processes.

Inhaled xenon is rapidly absorbed from the lungs. Borne by the circulation, it achieves reasonable concentrations in a variety of tissues within several seconds (*10, 13*). Imaging then depends on the survival of sufficient magnetization in the tissues of interest; i.e., the depolarization time constant, T_1, must be long in the lungs and blood. A T_1 of about 30 seconds has been measured for gaseous ^{129}Xe in excised mouse lungs (*1*). After adjusting for O_2 relaxivity (*14*) in a normally breathing subject, T_1 values are projected to be about 15 seconds in the lung (*1*). In early work, using xenon in thermal equilibrium, T_1 was measured to be roughly 40 seconds for ^{129}Xe dissolved in partly deoxygenated rat blood (*1*); an improved experiment yielded a lower limit of 10 s for T_1 in the plasma component of human venous blood (*15, 16*). We recently measured the T_1 for ^{129}Xe dissolved in fresh human blood (*17*). Using hyperpolarized ^{129}Xe reduces acquisition times from hours to seconds, minimizing blood degradation and sedimentation. T_1 was measured to be about 2.5 seconds in venous blood, and about 10 seconds in oxygenated blood (*17*). In the work of others (*2*), and more recently, of some of us (*18*), time constants ranging from 20–60 s have been observed in tissue resonances of live animals. Since inhaled xenon reaches equilibrium with the entire blood volume in about one blood circuit time [about 17 seconds from the antecubital vein in a human (*19, 20*)], we can expect significant accumulation of highly polarized ^{129}Xe in most tissues.

Hyperpolarized ^{129}Xe imaging of the lung may allow simultaneous investigation of both ventilation and perfusion. The seconds-long image-acquisition times should allow us to track the transport of ^{129}Xe from the lung to distal organs. HypX-MRI could supplement conventional MRI and other imaging modalities in three significant areas. (i) Imaging the pulmonary and cardiovascular system will be facilitated by this new technique because the polarization of ^{129}Xe will be high in the proximal circulation. HypX may also allow accurate measurements of blood flow in the brain and peripheral tissues. (ii) It should be possible to image the white matter of the brain using HypX-MRI, owing to xenon's high solubility in lipids, and the long relaxation times of the ^{129}Xe nucleus in such an environment. The short proton T_2 in the white matter has rendered membrane lipids essentially invisible to ^{1}H MRI (*21*). Xenon is twice as soluble in white matter as in gray matter, promising enhanced contrast (*13*). (iii) Easier imaging of brain functions may become possible with the development of HypX-MRI, since the ^{129}Xe signal may respond more directly and sensitively to metabolic changes in neural tissue. Increases in local blood flow and metabolism, arising from visual, olfactory, and tactile stimuli (*22, 23*), should produce detectable fluctuations in the hyperpolarized ^{129}Xe signal.

As soon as larger amounts of hyperpolarized xenon become available, we will begin to explore some of these possibilities.

ACKNOWLEDGMENTS

We thank Dilip Balamore for useful discussions on experimental approaches and Timothy Chupp, Kevin Coulter, and Matthew Rosen for assistance with ^{129}Xe polarization techniques. M.S.A. acknowledges financial support from the Whitaker Foundation. C.H.T., E.R.O., and R.L.W. acknowledge support from the Air Force Office of Scientific Research, the George W. Burch Foundation, and the Smithsonian Institution.

REFERENCES

1. M. Albert, G. Cates, B. Driehuys, W. Happer, B. Saam, C. S. Springer, and A. Wishnia, *Nature* 370, 199 (1994).
2. M. E. Wagshul, T. M. Button, H. F. Li, Z. Liang, and A. Wishnia, Abstracts of the Society of Magnetic Resonance, 3rd Annual Meeting, p. 1194, 1995.
3. H. Middleton, R. D. Black, B. Saam, G. D. Cates, G. P. Cofer, R. Guenther, W. Happer, L. W. Hedlund, G. A. Johnson, K. Juvan, and J. Swartz, *Magn. Reson. Med.* 33, 271 (1995).
4. G. A. Johnson, R. D. Black, G. Cates, G. Cofer, R. Gunther, W. Happer, L. W. Hedlund, H. Middleton, and J. Swartz, Abstracts of the Society of Magnetic Resonance, 3rd Annual Meeting, p. 392, 1995.
5. B. Driehuys, *Opt. Photonics News* 6(12), 38 (1995).
6. N. D. Bhaskar, W. Happer, and T. McClelland, *Phys. Rev. Lett.* 49, 25 (1982).
7. W. Happer, E. Miron, S. Schaefer, D. Schreiber, W. A. van Wijngaarden, and X. Zeng, *Phys. Rev. A* 29, 3092 (1984).
8. D. Raftery, H. Long, T. Meersmann, P. J. Grandinetti, L. Reven, and A. Pines, *Phys. Rev. Lett.* 66, 584 (1991).
9. G. D. Cates, R. J. Fitzgerald, A. S. Barton, P. Bogorad, M. Gatzke, N. R. Newbury, and B. Saam, *Phys. Rev. A* 45, 4631 (1992).
10. P. Weathersbee and L. Homer, *Undersea Biomed. Res.* 7, 277 (1980).
11. E. R. Oteiza, Ph.D. thesis, Harvard University, 1992.
12. M. Gatzke, G. D. Cates, B. Driehuys, D. Fox, W. Happer, and B. Saam, *Phys. Rev. Lett.* 70, 690 (1993).
13. B. E. Kendall and I. F. Moseley, *J. Neuroradiology* 8, 3 (1981).
14. C. J. Jameson, A. K. Jameson, and J. K. Hwang, *J. Chem. Phys.* 89, 4074 (1988).
15. M. Albert, V. Schepkin, and T. Budinger, Abstracts of the Society of Magnetic Resonance, 3rd Annual Meeting, p. 1193, 1995.

16. M. S. Albert, V. D. Schepkin, and T. F. Budinger, *J. Comp. Assist. Tomgr.* 19(6), 975 (1995).

17. M. S. Albert, D. Balamore, K. Sakai, D. Kacher, R. L. Walsworth, E. Oteiza, and F. A. Jolesz, Abstracts of the Society of Magnetic Resonance, 4th Annual Meeting, 1996.

18. K. Sakai, A. M. Bilek, C. H. Tseng, D. Balamore, R. L. Walsworth, E. Oteiza, F. A. Jolesz, and M. S. Albert, Abstracts of the Society of Magnetic Resonance, 4th Annual Meeting, 1996.

19. H. Susskind, K. J. Ellis, H. L. Atkins, S. H. Cohn, and P. Richards, *Prog. Nucl. Med.* 5, 13 (1978).

20. H. L. Blumgart and S. Weiss, *J. Clin. Invest.* 4, 339 (1927).

21. M. Barany, D. G. Spigos, E. Mok, P. N. Venkatasubramanian, A. C. Wilbur, and B. G. Langer, *Magn. Reson. Imaging* 5, 393 (1987).

22. K. K. Kwong, J. W. Belliveau, D. A. Chesler, I. E. Goldberg, R. M. Weisskoff, B. P. Poncelet, D. N. Kennedy, B. E. Hoppel, M. S. Cohen, R. Turner, H. M. Cheng, T. J. Brady, and B. R. Rosen, *Proc. Natl. Acad. Sci. USA* 89, 5675 (1992).

23. S. Ogawa, D. W. Tank, R. Menon, J. M. Ellermann, S.-G. Kim, H. Merkle, and K. Ugurbil, *Proc. Natl. Acad. Sci. USA* 89, 5951 (1992).